Title

Parallel-Reaction-Monitoring-Based Proteome-Wide Profiling of Differential Kinase Protein Expression during Prostate Cancer Metastasis in Vitro.

Journal

Analytical Chemistry, 91(15)

Authors

Yuan, Jun
Li, Lin
Wang, Yinsheng
et al.

Publication Date

2019-08-06

DOI

10.1021/acs.analchem.9b01561

Peer reviewed

HHS Public Access

Author manuscript

Anal Chem. Author manuscript; available in PMC 2020 August 06.

Published in final edited form as:

Anal Chem. 2019 August 06; 91(15): 9893–9900. doi:10.1021/acs.analchem.9b01561.

Parallel-Reaction-Monitoring-Based Proteome-Wide Profiling of Differential Kinase Protein Expression during Prostate Cancer Metastasis in Vitro

Weili Miao[†], **Jun Yuan**[‡], **Lin Li**[†], **Yinsheng Wang**[*,†]

[†]Department of Chemistry, University of California, Riverside, California 92521-0403, United States

[‡]Environmental Toxicology Program, University of California, Riverside, California 92521-0403, United States

Abstract

Prostate cancer is the most common type of cancer in men, and kinases are heavily pursued as drug targets for anticancer therapy. In this study, we applied our recently reported parallel-reaction-monitoring (PRM)-based targeted proteomic method to examine the reprogramming of the human kinome associated with bone metastasis of prostate cancer in vitro. The method displayed superior sensitivity over the shotgun-proteomic approach, and it facilitated the quantification of the relative expression of 276 kinase proteins in a pair of bone metastatic prostate cancer cells. Among the differentially expressed kinases, mitogen-activated protein kinase kinase kinase kinase 4 (MAP4K4) stimulates the migration and invasion of cultured prostate cancer cells, partially by modulating the activity of secreted matrix metalloproteinases 9 (MMP-9). We also found that the upregulation of MAP4K4 in metastatic prostate cancer cells is driven by the *MYC* proto-oncogene. Cumulatively, we identify MAP4K4 as a potential promoter for prostate cancer metastasis in vitro.

Graphical Abstract

[*]**Corresponding Author:** Y.W: tel, (951)827-2700; yinsheng.wang@ucr.edu.

Supporting Information

The following Supporting Information is available free of charge at ACS Web site : The Supporting Information is available free of charge on the ACS Publications website at DOI: 10.1021/acs.analchem.9b01561.

Relative expression levels of kinase proteins in PC3 and PC3MLN4 cells (XLSX)

Sequences for RT-qPCR primers, extracted-ion chromatograms for representative kinase peptides, KEGG pathway analysis of differentially expressed kinases, the comparison of mRNA levels of selected kinase genes (in normal, primary, and metastatic prostate cancer cells), Kaplan–Meier plot showing the relationship between the expression levels of *MAP4K4* genes and the overall survival of prostate cancer patients, Western blot results for confirming the shRNA-mediated knockdown of *MAP4K4* gene, the changes in migratory and invasive abilities of PC3 cells upon shRNA-mediated stable downregulation of MAP4K4, ChIP-seq data showing the occupancy of MYC protein in the promoter region of *MAP4K4*gene, and the effect of Myc on driving the expression of MAP4K4 in prostate cancer cells and patients (PDF)

The authors declare no competing financial interest.

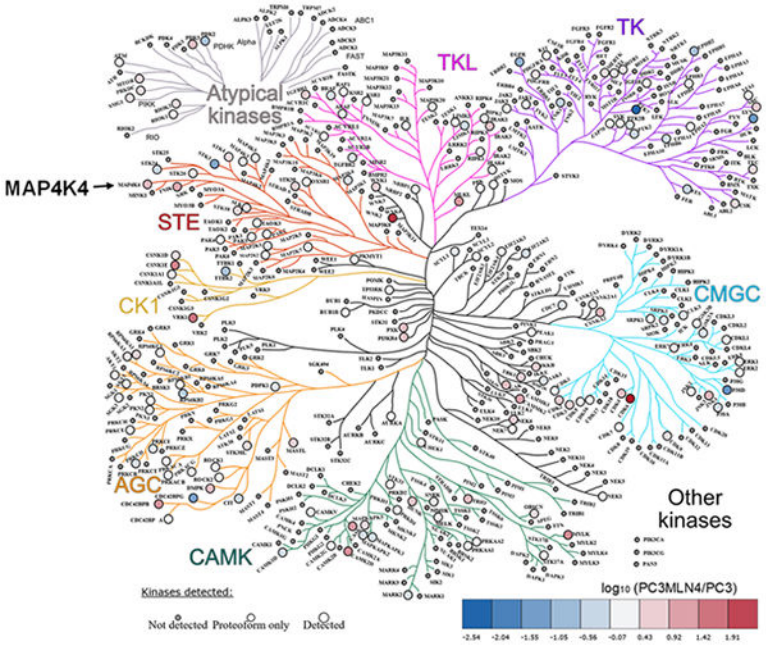

With nearly one in every seven men being diagnosed in their lifetime, prostate cancer (PCa) is a very common type of cancer in the United States.[1] Its metastases often appear years after primary treatment,[2,3] and 100% of those patients will eventually die from that.[4] Despite advances in prostate cancer screening, surgery, hormone-related therapy, and chemotherapy, ~27000 men still die of metastatic prostate cancer in the US each year.[5] Notably, autopsy results from patients showed that 100% of those who died from prostate cancer had bone metastases.[6] Thus, prostate cancer metastasis, particularly bone metastasis, is the major contributor to the high mortality rate in prostate cancer patients.

Recent studies have shown that aberrant kinase expression is associated with prostate cancer metastasis. Along this line, an in vivo screening of 125 candidate kinases led to the identification of 20 kinases with metastasis-promoting ability when they are expressed in murine prostate cells.[7] Among them, BMX was shown to be an important target for prostate cancer progression through regulating the mitogen-activated protein kinase (MAPK) pathway,[8] and BMX inhibitors have been extensively exploited for prostate cancer chemotherapy.[9] We reason that a comprehensive analysis of kinase protein expression during prostate cancer metastasis may offer a better understanding about the etiology of metastatic prostate cancer and yield novel targets for its therapeutic intervention.

Conventional quantitative analysis of the human kinome by mass spectrometry relies on the enrichment of kinases with the use of ATP-affinity probe or affinity resin immobilized with multiple kinase inhibitors.[10–16] However, the enrichment efficiency of a kinase with these methods can be influenced by not only the protein expression but also the activity of the kinase, thereby rendering it difficult to dissect the contributions of these two factors. To overcome this limitation, we recently introduced a targeted proteomics method, relying on parallel-reaction monitoring (PRM) and stable isotope labeling by amino acid in cell culture (SILAC), to analyze the kinase protein expression at the proteome-wide level.[17] In

particular, we developed a Skyline PRM kinome library, which encompassed 1050 unique tryptic peptides representing 478 distinct kinase proteins (395 protein kinases), on the basis of shotgun proteomic data collected for tryptic peptides of whole-cell protein lysates of multiple cell lines originating from different types of human tissues.[17–19]

In the current study, we employed the newly developed LC-PRM method to examine the differential expression of kinase proteins in a pair of bone metastasis prostate cancer cell lines. Our results led to the quantification of the relative expression of 276 unique kinases in the two lines of prostate cancer cells, and we identified MAP4K4 as a potential driver for prostate cancer metastasis in vitro.

EXPERIMENTAL SECTION

Cell Culture.

The PC3 cell line was originally derived from a bone metastasis of human prostatic adenocarcinoma origin, and PC3MLN4 was a metastasis-derived variant of PC3 (both lines were obtained from CCLC, MD Anderson Cancer Center).[20] In particular, PC3 cells were injected into the prostate and, after intraprostate growth, tumors from the prostate or lymph nodes were harvested and cancer cells were reinjected into the prostate; the cycle was repeated three to five times to generate PC3MLN4.[20] The cells were cultured in Dulbecco's modified Eagle medium (DMEM), which was supplemented with 10% fetal bovine serum (Invitrogen, Carlsbad, CA) and penicillin (100 IU/mL). The cells were maintained at 37 °C in a humidified atmosphere containing 5% CO_2. Approximately 2×10^7 cells were harvested, washed three times with cold PBS, and lysed by incubating on ice for 30 min with CelLytic M cell lysis reagent (Sigma) containing 1% protease inhibitor cocktail. The cell lysates were centrifuged at 9000*g* at 4 °C for 30 min, and the resulting supernatants were collected. For SILAC labeling experiments, the cells were cultured in SILAC medium containing unlabeled lysine and arginine or [$^{13}C_6$, $^{15}N_2$]-lysine and [$^{13}C_6$]-arginine for at least five cell doublings. The sequence for siMYC was 5′-GCUUGUACCUGCAGGAUCU-3′.

Lentiviral shMAP4K4.

All shRNA targeting sequences, which were designed according to Sigma (https://www.sigmaaldrich.com/life-science/functional-genomics-and-rnai/shrna/individual-genes.html), were cloned into pLKO.1-Puro (Addgene). The sequences for shMAP4K4 were 5′-TCCTTCCTGTTCCTCTTATAT-3′ (shMAP4K4–1), 5′-GAGAAAGATGAAACTGAGTAT-3′ (shMAP4K-2,) and 5′-CACCTATGGACAAGTCTATAA-3′ (shMAP4K4–3), and the scrambled control sequence was 5′-TCCTAAGGTTAAGTCGCCCTCG-3′.

Lentiviral particles were packaged using HEK293T cells. Virus-containing supernatants were collected at 48 h following transfection and filtered to eliminate cells. PC3 and PC3MLN4 cells were infected with the lentivirus for 48 h prior to puromycin (1.0 μg/mL) selection.

Tryptic Digestion of Whole-Cell Protein Lysates.

The protein lysates prepared from the aforementioned light and heavy SILAC-labeled PC3 cells were combined respectively with the heavy and light SILAC-labeled PC3MLN4 cells at a 1:1 ratio (in mass based on quantification from Bradford assay). Tryptic peptides for LC-PRM analysis were generated following the filter-aided sample preparation (FASP) protocol.[21] Approximately 50 μg of cell lysates was washed with 8 M urea for protein denaturation using a Microcon centrifugal filter with a molecular weight cutoff of 30 kDa, and the urea buffer was then removed by centrifugation at 10000 rpm. The ensuing denatured proteins were treated with dithiothreitol and iodoacetamide for cysteine reduction and alkylation, respectively. The proteins were subsequently digested with modified MS-grade trypsin (Pierce) at an enzyme/substrate ratio of 1/100 in 50 mM NH_4HCO_3 (pH 8.5) at 37 °C overnight. The resultant peptide mixture was dried in a Speed-vac, desalted with OMIX C18 pipet tips (Agilent Technologies), and subjected to LC-MS/MS analysis in the PRM mode. Samples from three replicates (two forward and one reverse SILAC labeling experiment) of lysates from the PC3/PC3MLN4 pair of prostate cancer cells were prepared for LC-PRM analyses.

LC-PRM Analysis.

All scheduled LC-PRM experiments were conducted on a Q Exactive Plus quadrupole-Orbitrap mass spectrometer coupled with an EASY-nLC 1200 system, as described recently.[22–24] The linear predictor of empirical RT from iRT[25] for targeted kinase peptides was determined by the linear regression of RT vs iRT of tryptic peptides of BSA obtained for the chromatography conditions prior to the analysis of kinase peptides.[22–24] This RT-iRT linear relationship was re-established between every eight LC-PRM runs by analyzing again the tryptic digestion mixture of BSA. The targeted precursor ions for all kinase peptides in the PRM kinome library for each sample were monitored in eight separate scheduled LC-PRM runs, where an 8 min retention time window was employed.

All raw files were processed in Skyline (version 3.5)[26] for the generation of extracted-ion chromatograms and for peak integration. Six most abundant y ions found in MS/MS acquired from shotgun proteomic analysis were selected for peptide identification and quantification, where a mass deviation of 20 ppm or less was imposed for fragment ions during the identification of peptides in Skyline. The targeted peptides were first manually checked to make sure that the chromatographic profiles of multiple fragment ions originating from the precursor ions of light and heavy forms of the same peptide exhibited the same elution time. The data were then processed to ensure that the distribution of the relative intensities of multiple transitions for the same precursor ion of kinase peptides is correlated with the theoretical distribution in the kinome MS/MS spectral library entry, with the dot product[27] value being larger than 0.7. The sum of peak areas from all transitions of light peptide and that for the corresponding heavy peptide were used for the relative quantification of the peptide.

All of the raw files and Skyline files for LC-PRM analyses of kinases for the paired metastatic prostate cancer cells were deposited into PeptideAtlas with the identifier number of PASS01318 (http://www.peptideatlas.org/PASS/PASS01318). The kinome library was

deposited into PeptideAtlas with the identifier number of PASS01178 (http://www.peptideatlas.org/PASS/PASS01178).

Bioinformatic Analysis of Publicly Available Data.

The mRNA expression levels of *MYC* and *MAP4K4* genes in 486 prostate cancer patients were retrieved from The Cancer Genome Atlas (TCGA) data using cBioPortal.[28] In addition, we analyzed the mRNA expression of *MAP4K4* gene in normal prostate and primary/metastatic prostate cancer tissues in the GSE6919 data set, which was downloaded from the NCBI Gene Expression Omnibus (GEO).[29,30] ChIP-seq data were retrieved from GSM935516.[31]

The Kaplan–Meier plot showing the correlation between patient survival and *MAP4K4* gene expression was generated using PROGgene (http://genomics.jefferson.edu/proggene/)[32] with the GSE16560 data set, which encompasses 281 prostate cancer patients.[33] The top 75% of expression values was considered as the high group. The kinase map in the TOC was generated using the online tool Peptracker (https://peptracker.com/epd/analytics/?show_plot).[34] KEGG pathway analysis was performed using DAVID functional annotation.[35,36]

Western Blot.

PC3 and PC3MLN4 cells were cultured in 6-well plates and lysed at 50–70% confluence following the aforementioned procedures. The concentrations of proteins in the resulting lysates were quantified using Bradford Assay (Bio-Rad). The whole-cell lysate for each sample (10 μg) was denatured by boiling in Laemmli loading buffer and resolved by SDS-PAGE. The proteins were subsequently transferred onto a nitrocellulose membrane at 4 °C overnight. The resulting membrane was blocked with PBS-T (PBS with 0.1% Tween 20) containing 5% milk (Bio-Rad) at 4 °C for 6 h. The membrane was incubated, at 4 °C, with primary antibody overnight and then with secondary antibody at room temperature for 1 h. After thorough washing with PBS-T, the HRP signals were detected using Pierce ECL Western Blotting Substrate (Thermo).

Antibodies recognizing human AK1 (Santa Cruz Biotechnology, sc-165981, 1/1000 dilution), ARAF (Santa Cruz Biotechnology, sc-166771, 1/4000 dilution), EGFR (Santa Cruz Biotechnology, sc-03, 1/10000 dilution), and MAP4K4 (ProteinTech, 55247–1-AP, 1/2000 dilution) were employed as the primary antibodies for Western blot analysis. Horseradish peroxidase conjugated anti-rabbit IgG and IRDye 680LT Goat anti-Mouse IgG (H+L) were used as secondary antibodies. Membranes were also probed with anti-actin antibody (Cell Signaling #4967, 1/10000 dilution) to validate equal loading of protein lysate.

Migration and Invasion Assays.

Migration and invasion assays were performed using a Matrigel Transwell Chamber (Corning) containing 8 μm pore polycarbonate filters.[37] In the migration assay, the harvested PC3 and PC3MLN4 cells, suspended in 100 μL of serum-free medium at final concentrations of 4×10^5 and 1×10^6 cells/mL, respectively, were dispersed to the top chamber of the Transwell setup, whereas the bottom chamber contained medium with 10%

FBS. After incubation for 24 h (for PC3 cells) or 48 h (for PC3MLN4 cells), non-migrated cells and media in the top chamber were removed by using a cotton swab and the migrated cells on the bottom surface of the insert membrane were fixed by incubating with 75% methanol at room temperature for 15 min. The cells were then stained with 0.2% crystal violet in 10% ethanol for 15 min. After washing and drying, the insert membranes were imaged under a light microscope. As the same number of cells was initially suspended in each well, cell migration was reported as the number of migrated cells.

The invasion assay was conducted similarly, with the exception that 200–400 μg/mL Matrigel in serum-free media was coated on the top chamber of the filter and the medium with Matrigel was removed after a 2 h incubation at 37 °C. The cells were then dispersed, stained, and counted, as noted above for the migration assay. Cell invasion was determined on the basis of the ratio of the number of invaded cells over that of the migrated cells.

Gelatin Zymography Assay.

Concentrated medium collected from cultured prostate cancer cells was loaded without reduction onto a 10% SDS-PAGE gel with 0.1% gelatin. After electrophoresis under non-reducing conditions, the gels were washed with 2.5% Triton X-100 (Sigma) to remove SDS and to renature the MMP-2 and MMP-9 proteins. The gels were subsequently incubated in the developing buffer (50 mM Tris-HCl, pH 7.5, 1% Triton X-100, 5 mM $CaCl_2$, and 1 μM $ZnCl_2$) overnight to induce gelatin lysis by the renatured MMP-2 and MMP-9. The gel bands at approximately 63 and 82 kDa were attributed to MMP-2 and MMP-9, respectively.[38] The relative amounts of active MMP-2 and MMP-9 were then quantified on the basis of their band intensities with the use of ImageJ.[39]

Real-Time PCR.

Cells were seeded in 6-well plates at the 50–70% confluence level. Total RNA was extracted from cells using TRI Reagent (Sigma). Approximately 3 μg of RNA was reverse transcribed by employing M-MLV reverse transcriptase (Promega) and an oligo$(dT)_{18}$ primer. After a 60 min incubation at 42 °C, the reverse transcriptase was deactivated by heating at 75 °C for 5 min. Real-time quantitative PCR was performed using an iQ SYBR Green Supermix kit (Bio-Rad) on a Bio-Rad iCycler system (Bio-Rad), and the running conditions were at 95 °C for 3 min and 45 cycles at 95 °C for 15 s, 55 °C for 30 s, and 72 °C for 45 s. Relative levels of gene expression were quantified using the comparative cycle threshold (Ct) method (ΔΔCt),[40] and the primer sequences are given in Table S2.

RESULTS AND DISCUSSION

Differential Expression of Kinases in Bone Metastatic Human Prostate Cancer Cells.

We sought to investigate the roles of specific kinases during bone metastasis of prostate cancer in vitro. Toward this end, we employed SILAC,[41] in conjunction with an LC-PRM-based targeted kinome profiling method,[17] to examine the differential expression of kinases in a pair of metastatic prostate cancer cells: i.e., PC3 and PC3MLN4 (Figure 1a). PC3 cells were derived from bone metastasis of prostate cancer, and PC3MLN4 cells were metastasis-derived variants of PC3. PC3 cells were harvested after intraprostate growth and reinjected

into the prostate to obtain the bone metastatic cell line. This cycle was repeated three to five times to yield the bone metastatic cell line PC3MLN4. In comparison to PC3 cells, PC3MLN4 cells were found to produce enhanced regional lymph node and distant organ metastasis in an animal model.[20]

By utilizing the PRM-based targeted proteomic method, we were able to quantify 276 unique kinases in the PC3MLN4/PC3 pair of metastatic prostate cancer cells (Figures 1b and 2 and Table S1). The failure in detecting the rest of the kinases in the PRM spectral library, which encompassed a total of 478 kinases, is likely due to their relatively low levels of expression in the cultured prostate cancer cells employed in the present study. For comparison, we analyzed the same samples by employing LC-MS/MS in data-dependent acquisition (DDA) mode. As shown in Figure 1b, DDA analyses only led to the identification of 31 kinases in the two forward and one reverse SILAC labeling sample (Figure 1b). Additionally, the PRM method afforded reliable and reproducible data, where all PRM transitions (four to six transitions) employed for kinase peptide quantification exhibited the same retention time and displayed dot product (dotp)[27] values of >0.7 (Figure S1). In particular, the ratios obtained from forward and reverse SILAC labeling experiments are consistent (R^2 = 0.72, Figure 1c,d and Table S1). Furthermore, the relative standard deviations (RSD) for kinase protein quantification was 15.5% for the matched pair of cell lines, indicating the robustness of protein quantification with this method (Table S1). We also monitored the relative expression levels for four of the quantified kinase proteins (EGFR, MAP4K4, ARAF, AK1) in PC3 and PC3MLN4 cells using Western blot analyses (Figure 3a–c), which validated the proteomic data. Hence, the LC-PRM method, together with SILAC, provided accurate quantification of kinase protein expression.

We found that, among the 276 quantified kinases, 71 and 62 were up- and downregulated, respectively, by at least 1.5-fold in PC3MLN4 relative to PC3 metastatic prostate cancer cells. Kyoto Encyclopedia of Genes and Genomes (KEGG) pathway analysis revealed prostate cancer as one of the upregulated pathways (Figure S2). Among the 71 kinases upregulated in the more metastatic PC3ML4 cells, MERTK and SRC were previously shown to promote prostate cancer bone metastasis and are highly expressed in human metastatic prostate cancer tissues,[7,42] substantiating the capability of our quantitative proteomic method in identifying putative drivers of prostate cancer metastasis.

MAP4K4 Drives Prostate Cancer Metastasis in Vitro through Modulating the Activity of MMP-9.

We then investigated whether the differential expression of these kinase proteins in the paired PC3/PC3MLN4 cells are correlated with their respective mRNA expression levels in prostate cancer patients with different degrees of disease progression. An analysis of the GSE6919 data set collected from 168 individuals (77 normal, 66 primary, and 25 metastatic prostate cancer) revealed significantly elevated expressions of *CSNK1E*, *CAMK2D*, *TRIO*, *PXK*, *PHKB*, and *MAP4K4* genes and reduced expression of *STK24* gene in the metastatic prostate cancer tissues, in comparison to normal prostate or primary prostate cancer tissues (Figure 3d and Figures S3 and S4 for representative genes whose differential expression are not positively correlated with survival of prostate cancer patients).[29,30]

Among the 6 kinases that are upregulated in the more metastatic PC3MLN4 cells, only MAP4K4 is correlated with prostate cancer patient survival. In this vein, Kaplan–Meier survival analysis of the data retrieved from 281 prostate cancer patients revealed a significant correlation between higher levels of mRNA expression of *MAP4K4* gene and poorer prognosis (Figure S5).[33] Additionally, elevated MAP4K4 expression was significantly correlated with poorer overall and recurrence-free survival and associated with a higher frequency of recurrence/metastasis, larger tumor size, and increased number of positive lymph nodes in pancreatic cancer patients.[43] Likewise, higher levels of mRNA expression of *MAP4K4* gene contribute to augmented proliferation and invasion of ovarian cancer and pancreatic cancer cells.[44,45] Moreover, a previous small interferencing RNA (siRNA) screen for modulators of tumor cell motility led to the identification of MAP4K4 as a promigratory kinase, where siRNA-mediated knockdown of MAP4K4 led to diminished migratory capacity for several cell lines, including DU-145 prostate cancer cell line.[45] Together, these previously published studies suggested that MAP4K4 plays an important role in cancer progression.

Next, we investigated the potential roles of MAP4K4 in prostate cancer metastasis by analyzing how the migration and invasion capacities of prostate cancer cells are influenced by the expression levels of MAP4K4.[37] Our results from transwell assays demonstrated that the migratory and invasive abilities of PC3 and PC3MLN4 bone metastatic prostate cancer cells were suppressed upon shRNA-mediated stable knockdown of MAP4K4 (Figure 4 and Figure S6).

Degradation of extracellular matrix proteins is known to be important in promoting metastatic transformation, and such degradation requires matrix metalloproteinases (MMP), particularly MMP-2 and MMP-9.[46] By employing a gelatin zymography assay, we investigated the modulations of enzymatic activities of MMP-2 and MMP-9 by the expression level of MAP4K4. It turned out that the activity of secreted MMP-9 was diminished in PC3 and PC3MLN4 metastatic prostate cancer cells upon stable knockdown of MAP4K4 (Figure 5),[39] though the activity of secreted MMP-2 is not positively modulated by MAP4K4 (Figure 5). Moreover, previous studies showed that, among the MMPs, MMP-9 plays a significant role in prostate cancer bone metastasis.[47,48] Together, the above results lend evidence to support the notion that MAP4K4 may drive prostate cancer metastasis in vitro, at least in part, through modulating the activity of MMP-9.

MAP4K4 and MYC.

MYC, one of the most potent protooncogenes,[49,50] can promote tumorigenesis in various organs, and prostate cancer patients display augmented expression of MYC at both the mRNA and protein levels.[51,52] Owing to the effect of MYC on carcinogenesis, proteins which interact in the same pathway often also have a role in cancer progression. An analysis of the previously published ChIP-Seq data revealed the occupancy of MYC transcription factor in the promoter region of *MAP4K4* gene (Figure S7).[31] Therefore, we decided to examine whether elevated expression of MAP4K4 in the more metastatic PC3MLN4 cells emanates from upregulation by the *MYC* proto-oncogene. Our real-time qPCR results revealed augmented mRNA expression of *MAP4K4* gene in PC3MLN4 relative to PC3 cells

(Figure S8a), suggesting that the increased expression of MAP4K4 protein in PC3MLN4 cells arises from its transcriptional up-regulation. Moreover, siRNA-mediated knockdown of *MYC* led to pronounced attenuation in mRNA expression of *MAP4K4* gene in PC3MLN4 prostate cancer cells, though a slight drop in MAP4K4 mRNA expression was also observed in PC3 cells (Figure S8b). We further analyzed the mRNA expression levels of *MAP4K4* and *MYC* genes in 486 prostate cancer patients included in the TCGA database from cBioportal,[53] and we found a strong correlation between mRNA expression levels of these two genes (Figure S8c), indicating that *MYC* may regulate the expression of *MAP4K4* gene in prostate cancer cells and patients.

We further investigated the underlying mechanism of elevated transcriptional regulation of MAP4K4 in metastatic prostate cancer cells by interrogating the promoter methylation status of *MAP4K4* gene. DNA methylation at CpG dinucleotide sites in promoters is closely linked with downstream gene repression because such methylation impairs transcription factor binding.[54] Along this line, an analysis of the promoter methylation of *MAP4K4* gene in the 486 prostate cancer patients revealed that lower levels of methylation are significantly correlated with higher levels of its mRNA expression (Figure S8d). This result suggests that the augmented expression of *MAP4K4* in metastatic prostate cancer patients could be modulated by *MYC* via an epigenetic mechanism.

CONCLUSIONS

In this study, we employed a recently developed PRM-based targeted proteomic method for examining the differential expression of kinase proteins in a pair of bone metastatic prostate cancer cells. We were able to quantify 276 kinases, and 133 of them were differentially expressed by at least 1.5-fold in the two lines of prostate cancer cells. Importantly, we found that one of the differentially expressed kinases, MAP4K4, promotes the migration and invasion of cultured prostate cancer cells through regulating the activities of secreted MMP-9. Moreover, our work supports a role of *MYC* proto-oncogene in upregulating the *MAP4K4* gene expression in metastatic prostate cancer patients. Overall, our study reveals MAP4K4 as a potential driver for prostate cancer metastasis in vitro.

Supplementary Material

Refer to Web version on PubMed Central for supplementary material.

ACKNOWLEDGMENTS

This work was supported by the National Institutes of Health (R01 CA210072). The authors also thank Dr. Nathan E. Price for reading and editing this manuscript.

REFERENCES

(1). Kim EH; Andriole GL Mo. Med 2018, 115, 131. [PubMed: 30228703]
(2). Ruppender NS; Morrissey C; Lange PH; Vessella RL Cancer Metastasis Rev 2013, 32, 501–509. [PubMed: 23612741]
(3). Lam H-M; Vessella RL; Morrissey C Drug Discovery Today: Technol 2014, 11, 41–47.

(4). van der Toom EE; Axelrod HD; de la Rosette JJ; de Reijke TM; Pienta KJ; Valkenburg KC Nat. Rev. Urol 2019, 16, 7–22. [PubMed: 30479377]

(5). Siegel RL; Miller KD; Jemal A Ca-Cancer J. Clin 2015, 65, 5–29. [PubMed: 25559415]

(6). Mehra R; Kumar-Sinha C; Shankar S; Lonigro RJ; Jing X; Philips NE; Siddiqui J; Han B; Cao X; Smith DC; Shah RB; Chinnaiyan AM; Pienta KJ Clin. Cancer Res 2011, 17, 3924–3932. [PubMed: 21555375]

(7). Faltermeier CM; Drake JM; Clark PM; Smith BA; Zong Y; Volpe C; Mathis C; Morrissey C; Castor B; Huang J; Witte ON Proc. Natl. Acad. Sci. U. S. A 2016, 113, E172. [PubMed: 26621741]

(8). Dai B; Kim O; Xie Y; Guo Z; Xu K; Wang B; Kong X; Melamed J; Chen H; Bieberich CJ; Borowsky AD; Kung H-J; Wei G; Ostrowski MC; Brodie A; Qiu Y Cancer Res 2006, 66, 8058–8064. [PubMed: 16912182]

(9). Liu F; Zhang X; Weisberg E; Chen S; Hur W; Wu H; Zhao Z; Wang W; Mao M; Cai C; Simon NI; Sanda T; Wang J; Look AT; Griffin JD; Balk SP; Liu Q; Gray NS ACS Chem. Biol 2013, 8, 1423–1428. [PubMed: 23594111]

(10). Miao W; Xiao Y; Guo L; Jiang X; Huang M; Wang Y Anal. Chem 2016, 88, 9773–9779. [PubMed: 27626823]

(11). Xiao Y; Guo L; Wang Y Mol. Cell. Proteomics 2014, 13, 1065–1075. [PubMed: 24520089]

(12). Patricelli MP; Szardenings AK; Liyanage M; Nomanbhoy TK; Wu M; Weissig H; Aban A; Chun D; Tanner S; Kozarich JW Biochemistry 2007, 46, 350–358. [PubMed: 17209545]

(13). Duncan JS; Whittle MC; Nakamura K; Abell AN; Midland AA; Zawistowski JS; Johnson NL; Granger DA; Jordan NV; Darr DB; Usary J; Kuan PF; Smalley DM; Major B; He X; Hoadley KA; Zhou B; Sharpless NE; Perou CM; Kim WY; Gomez SM; Chen X; Jin J; Frye SV; Earp HS; Graves LM; Johnson GL Cell 2012, 149, 307–21. [PubMed: 22500798]

(14). Stuhlmiller TJ; Miller SM; Zawistowski JS; Nakamura K; Beltran AS; Duncan JS; Angus SP; Collins KA; Granger DA; Reuther RA; Graves LM; Gomez SM; Kuan PF; Parker JS; Chen X; Sciaky N; Carey LA; Earp HS; Jin J; Johnson GL Cell Rep 2015, 11, 390–404. [PubMed: 25865888]

(15). Oppermann FS; Gnad F; Olsen JV; Hornberger R; Greff Z; Kéri G; Mann M; Daub H Mol. Cell. Proteomics 2009, 8, 1751–1764. [PubMed: 19369195]

(16). Urisman A; Levin RS; Gordan JD; Webber JT; Hernandez H; Ishihama Y; Shokat KM; Burlingame AL Mol. Cell. Proteomics 2017, 16, 265–277. [PubMed: 27940637]

(17). Miao W; Guo L; Wang Y Anal. Chem 2019, 91, 3209–3214. [PubMed: 30773012]

(18). Miao W; Wang YJ Proteome Res 2019, 18, 2279–2286.

(19). Miao W; Wang YJ Proteome Res 2019, 18, 2624–2631.

(20). Wu X; Gong S; Roy-Burman P; Lee P; Culig Z Endocr.-Relat. Cancer 2013, 20, R155–R170. [PubMed: 23580590]

(21). Wiśniewski JR; Zougman A; Nagaraj N; Mann M Nat. Methods 2009, 6, 359–362. [PubMed: 19377485]

(22). Miao W; Li L; Wang Y Anal. Chem 2018, 90, 6835–6842. [PubMed: 29722524]

(23). Miao W; Li L; Wang Y Anal. Chem 2018, 90, 11751–11755. [PubMed: 30247883]

(24). Miao W; Fan M; Huang M; Li JJ; Wang Y Chem. Res. Toxicol 2019, 32, 326–332. [PubMed: 30596229]

(25). Escher C; Reiter L; MacLean B; Ossola R; Herzog F; Chilton J; MacCoss MJ; Rinner O Proteomics 2012, 12, 1111–1121. [PubMed: 22577012]

(26). MacLean B; Tomazela DM; Shulman N; Chambers M; Finney GL; Frewen B; Kern R; Tabb DL; Liebler DC; MacCoss MJ Bioinformatics 2010, 26, 966–968. [PubMed: 20147306]

(27). de Graaf EL; Altelaar AF; van Breukelen B; Mohammed S; Heck AJ J. Proteome Res. 2011, 10, 4334–4341. [PubMed: 21726076]

(28). Cerami E; Gao J; Dogrusoz U; Gross BE; Sumer SO; Aksoy BA; Jacobsen A; Byrne CJ; Heuer ML; Larsson E; Antipin Y; Reva B; Goldberg AP; Sander C; Schultz N Cancer Discovery 2012, 2, 401–404. [PubMed: 22588877]

(29). Chandran UR; Ma C; Dhir R; Bisceglia M; Lyons-Weiler M; Liang W; Michalopoulos G; Becich M; Monzon FA BMC Cancer 2007, 7, 64. [PubMed: 17430594]

(30). Yu YP; Landsittel D; Jing L; Nelson J; Ren B; Liu L; McDonald C; Thomas R; Dhir R; Finkelstein S; Michalopoulos G; Becich M; Luo J-HJ Clin. Oncol 2004, 22, 2790–2799.

(31). The Encode Project Consortium. Nature 2012, 489, 57–74. [PubMed: 22955616]

(32). Goswami CP; Nakshatri HJ Clin. Bioinf 2013, 3, 22.

(33). Sboner A; Demichelis F; Calza S; Pawitan Y; Setlur SR; Hoshida Y; Perner S; Adami H-O; Fall K; Mucci LA; Kantoff PW; Stampfer M; Andersson S-O; Varenhorst E; Johansson J-E; Gerstein MB; Golub TR; Rubin MA; Andrén O BMC Med. Genomics 2010, 3, 8. [PubMed: 20233430]

(34). Brenes A; Lamond AI Bioinformatics 2019, 35, 1441–1442. [PubMed: 30239567]

(35). Huang DW; Sherman BT; Lempicki RA Nat. Protoc 2009, 4, 44–57. [PubMed: 19131956]

(36). Huang DW; Sherman BT; Lempicki RA Nucleic Acids Res 2009, 37, 1–13. [PubMed: 19033363]

(37). Albini A; Benelli R Nat. Protoc 2007, 2, 504–511. [PubMed: 17406614]

(38). Tajhya RB; Patel RS; Beeton C Methods Mol. Biol 2017, 1579, 231–244. [PubMed: 28299740]

(39). Vandooren J; Geurts N; Martens E; Van den Steen PE; Opdenakker G Nat. Methods 2013, 10, 211–220. [PubMed: 23443633]

(40). Livak KJ; Schmittgen TD Methods 2001, 25, 402–408. [PubMed: 11846609]

(41). Ong S-E; Blagoev B; Kratchmarova I; Kristensen DB; Steen H; Pandey A; Mann M Mol. Cell. Proteomics 2002, 1, 376–386. [PubMed: 12118079]

(42). Park SI; Zhang J; Phillips KA; Araujo JC; Najjar AM; Volgin AY; Gelovani JG; Kim S-J; Wang Z; Gallick GE Cancer Res 2008, 68, 3323–3333. [PubMed: 18451159]

(43). Liang JJ; Wang H; Rashid A; Tan T-H; Hwang RF; Hamilton SR; Abbruzzese JL; Evans DB; Wang H Clin. Cancer Res 2008, 14, 7043–7049. [PubMed: 18981001]

(44). Zhao G; Wang B; Liu Y; Zhang J.-g.; Deng S.-c.; Qin Q; Tian K; Li X; Zhu S; Niu Y; Gong Q; Wang C.-y. Mol. Cancer Ther 2013, 12, 2569–2580. [PubMed: 24013097]

(45). Collins CS; Hong J; Sapinoso L; Zhou Y; Liu Z; Micklash K; Schultz PG; Hampton GM Proc. Natl. Acad. Sci. U. S. A 2006, 103, 3775–3780. [PubMed: 16537454]

(46). Bauvois B Biochim. Biophys. Acta, Rev. Cancer 2012, 1825, 29–36.

(47). Muñoz D; Serrano MK; Hernandez ME; Haller R; Swanson T; Slaton JW; Sinha AA; Wilson MJ Exp. Mol. Pathol 2017, 103, 300–305. [PubMed: 29175302]

(48). Pego ER; Fernández I; Núñez MJ Urol Oncol-Semin. Ori 2018, 36, 272–282.

(49). Stone J; de Lange T; Ramsay G; Jakobovits E; Bishop JM; Varmus H; Lee W Mol. Cell. Biol 1987, 7, 1697–1709. [PubMed: 3299053]

(50). Hemann MT; Bric A; Teruya-Feldstein J; Herbst A; Nilsson JA; Cordon-Cardo C; Cleveland JL; Tansey WP; Lowe SW Nature 2005, 436, 807–811. [PubMed: 16094360]

(51). Pettersson A; Gerke T; Penney KL; Lis RT; Stack EC; Pértega-Gomes N; Zadra G; Tyekucheva S; Giovannucci EL; Mucci LA; Loda M Cancer Epidemiol., Biomarkers Prev 2018, 27, 201–207. [PubMed: 29141848]

(52). Hawksworth D; Ravindranath L; Chen Y; Furusato B; Sesterhenn IA; McLeod DG; Srivastava S; Petrovics G Prostate Cancer Prostatic Dis 2010, 13, 311–315. [PubMed: 20820186]

(53). Gao J; Aksoy BA; Dogrusoz U; Dresdner G; Gross B; Sumer SO; Sun Y; Jacobsen A; Sinha R; Larsson E; Cerami E; Sander C; Schultz N Sci. Signaling 2013, 6, No. pl1.

(54). Medvedeva YA; Khamis AM; Kulakovskiy IV; Ba-Alawi W; Bhuyan MSI; Kawaji H; Lassmann T; Harbers M; Forrest ARR; Bajic VB BMC Genomics 2014, 15, 119. [PubMed: 24669864]

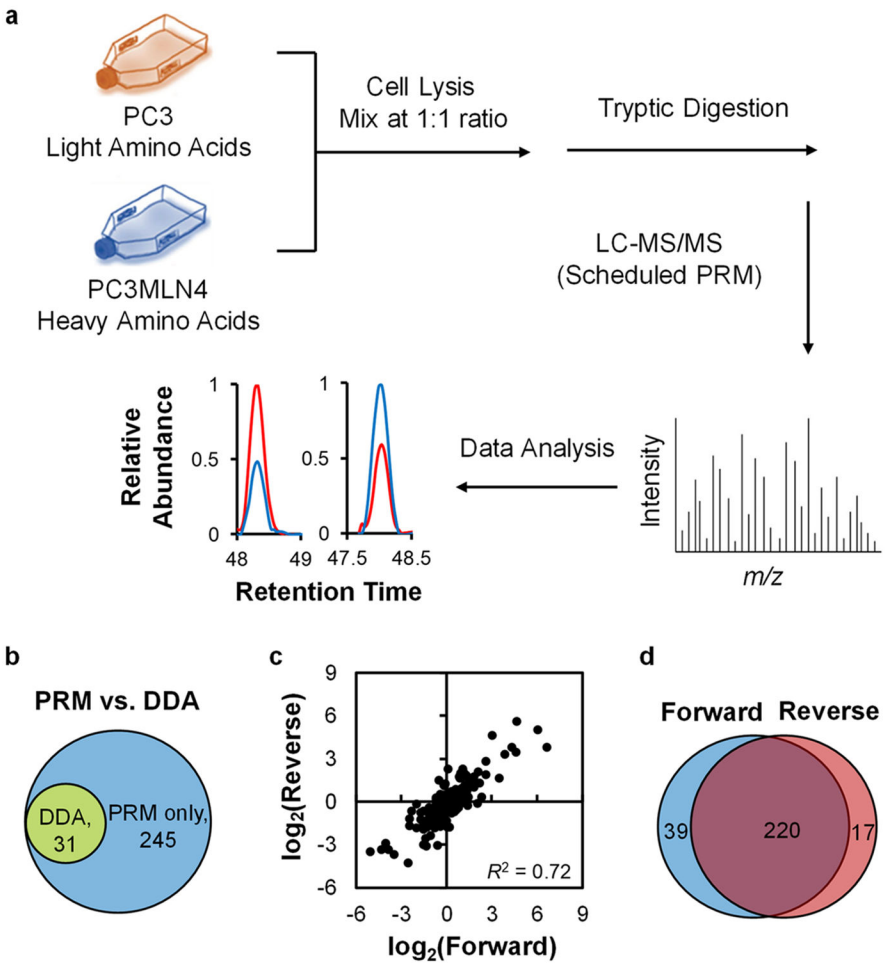

Figure 1.

PRM-based targeted proteomic approach for quantifying the differential expression of kinase proteins in a pair of metastatic prostate cancer cells. (a) Experimental strategy for the PRM-based targeted proteomic approach, involving the use of forward SILAC labeling. (b) A Venn diagram displaying the overlap between quantified kinases obtained from PRM analyses and DDA analyses. (c) Correlation between the ratios of kinase protein expression in PC3/PC3MLN4 cells obtained from forward and reverse SILAC labeling experiments. (d) A Venn diagram displaying the overlap between quantified kinases from the forward and reverse SILAC labeling experiments of the PC3/PC3MLN4 pair of prostate cancer cells.

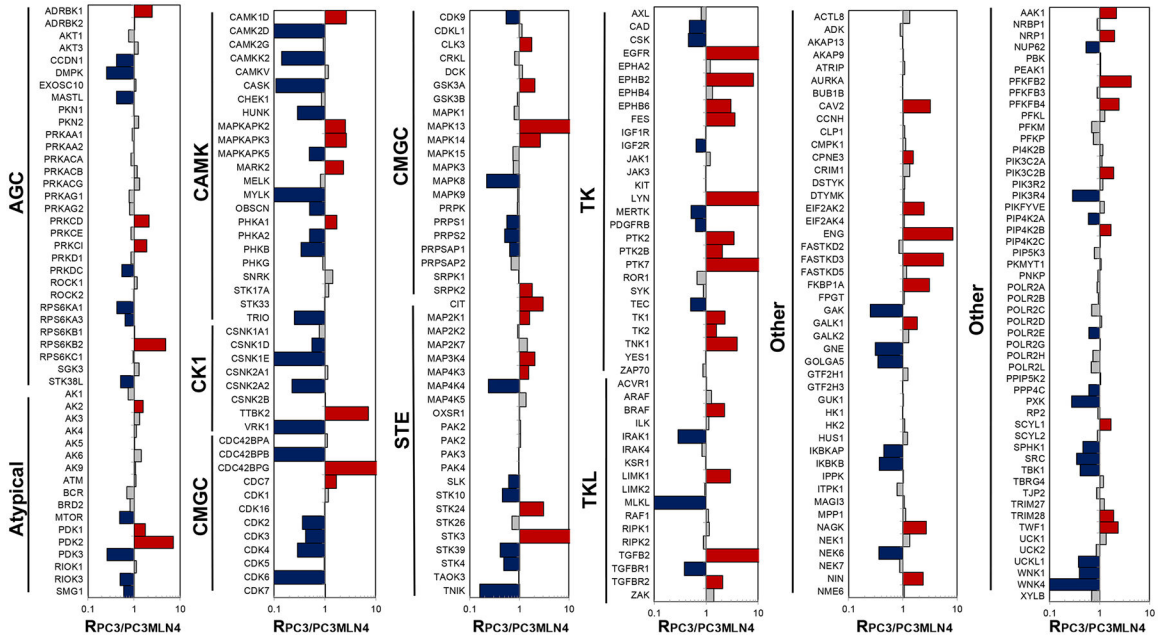

Figure 2.

Differential expression of kinase proteins in the matched pair of PC3/PC3MLN4 cells. The data were calculated from the means of two forward and one reverse SILAC labeling experiment (see Table S1 for ratios obtained from individual measurements). Blue, red, and gray bars represent those kinases with ratios (PC3/PC3MLN4) being <0.67, >1.5, and between 0.67 and 1.5, respectively.

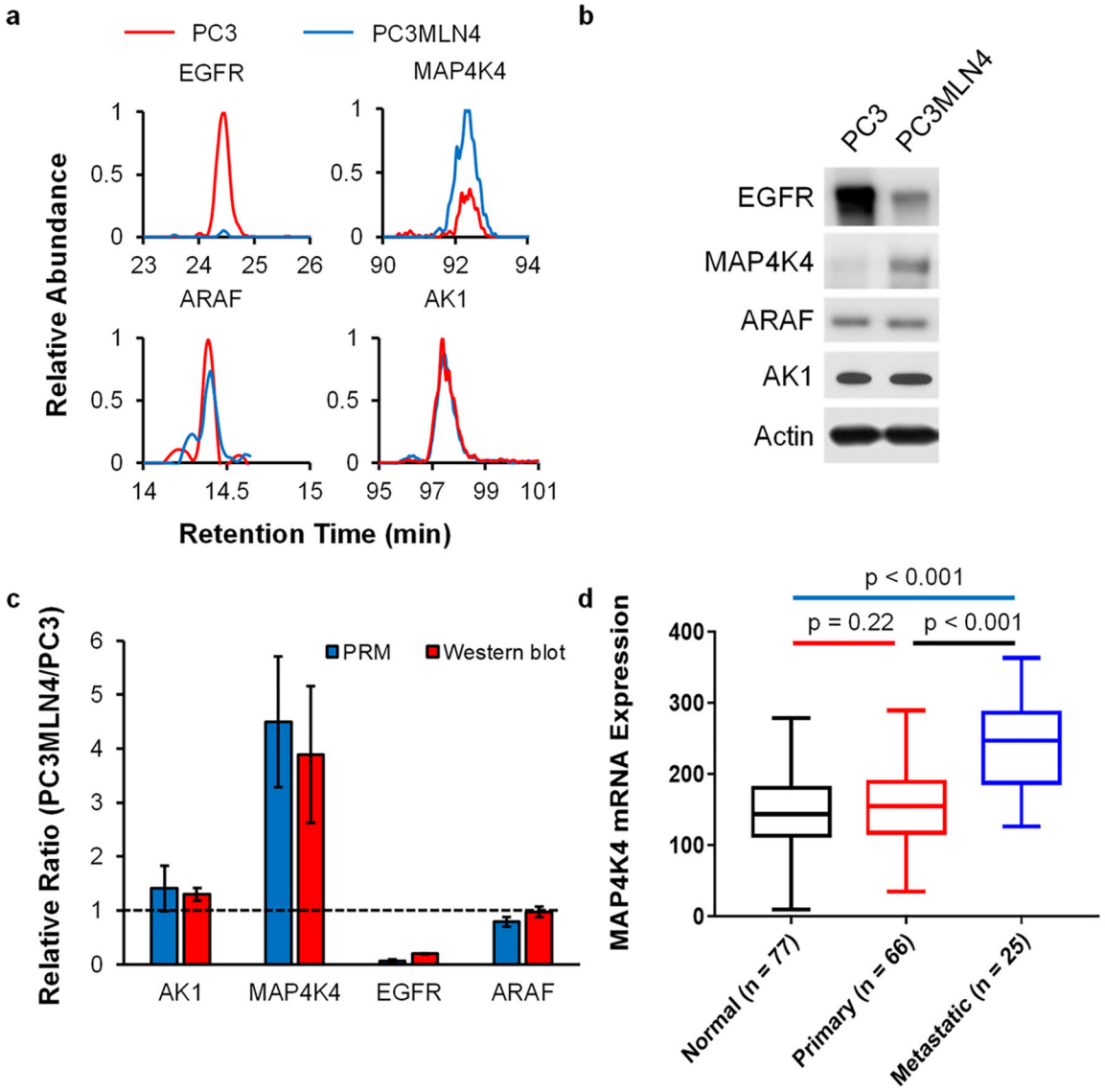

Figure 3.

Western blot validation of the relative expression levels of kinases in the paired metastatic prostate cancer cells. (a) PRM traces for the quantifications of EGFR, MAP4K4, ARAF, and AK1 proteins in PC3/PC3MLN4 cells. (b) Western blot for the validation of the relative expression levels of EGFR, MAP4K4, ARAF, and AK1 proteins in the paired prostate cancer cells. (c) Quantitative comparison of the ratios of EGFR, MAP4K4, ARAF, and AK1 in PC3MLN4/PC3 cells obtained from PRM and Western blot analysis. The data represent the mean ± SD of the quantification results ($n = 3$). (d) Box-and-whisker plot showing the comparison of mRNA levels of *MAP4K4* gene in normal prostate and primary/metastatic prostate cancer tissues. Data were retrieved from 168 prostate cancer patients from the GSE6919 data set. Shown by the whiskers extending outside of the box are the maximum and minimum mRNA levels of MAP4K4 expression from prostate cancer patients. The displayed boxes contain the interquartile mRNA level of MAP4K4 expression obtained from prostate cancer patients.

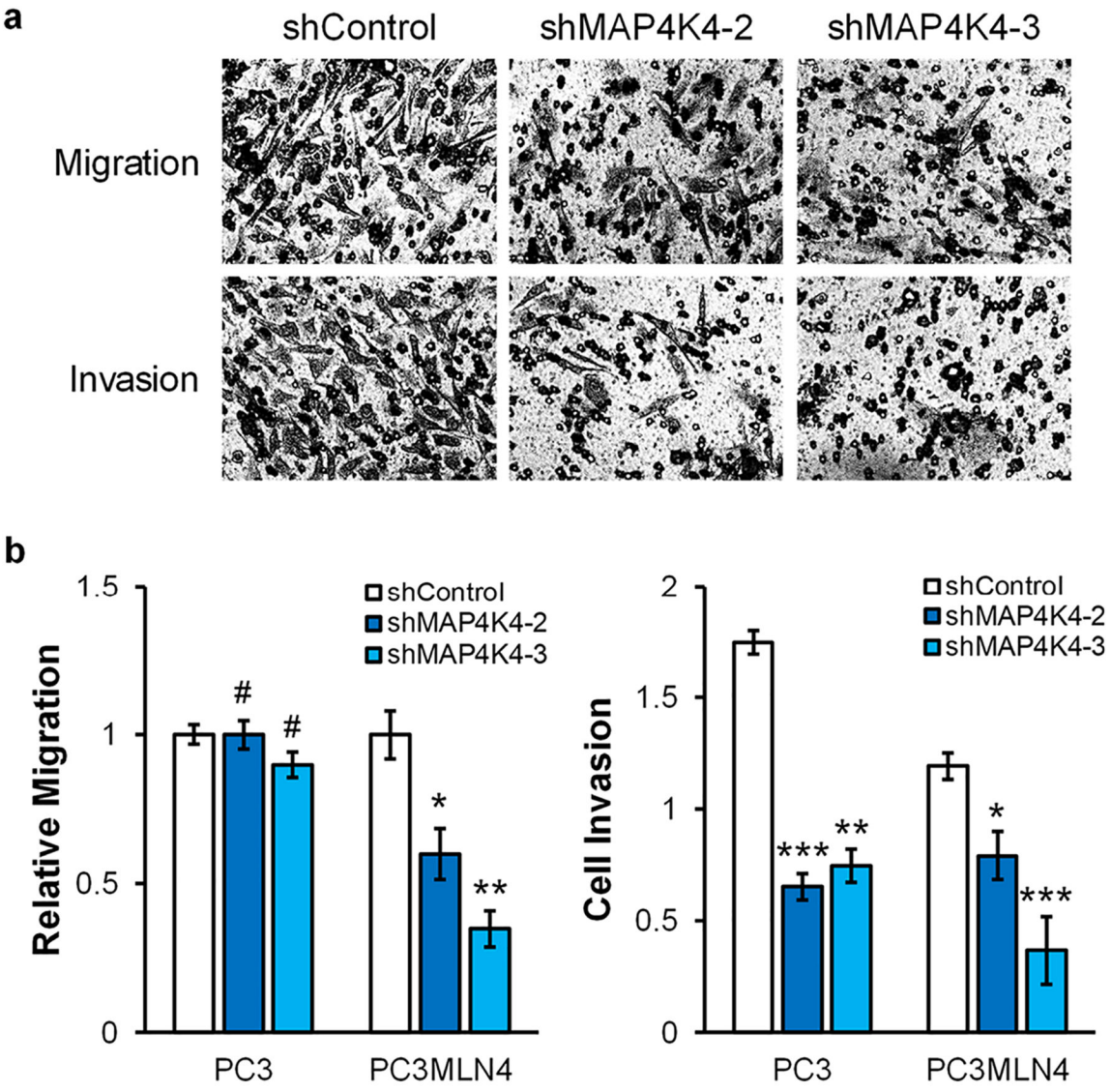

Figure 4.

MAP4K4 modulates the migratory and invasive capacities of metastatic prostate cancer cells. (a) The migratory and invasive abilities of PC3MLN4 cells upon shRNA-mediated stable knockdown of *MAP4K4* gene. (b) Quantification results of migratory and invasive abilities of PC3 and PC3MLN4 cells upon shRNA-mediated stable knockdown of *MAP4K4* gene. The data represent the mean ± SD of the quantification results ($n = 3$). The p values were calculated on the basis of an unpaired, two-tailed Student's t test: #, $p \geq 0.05$; *, $0.01 \leq p < 0.05$; **, $0.001 \leq p < 0.01$; ***, $p < 0.001$.

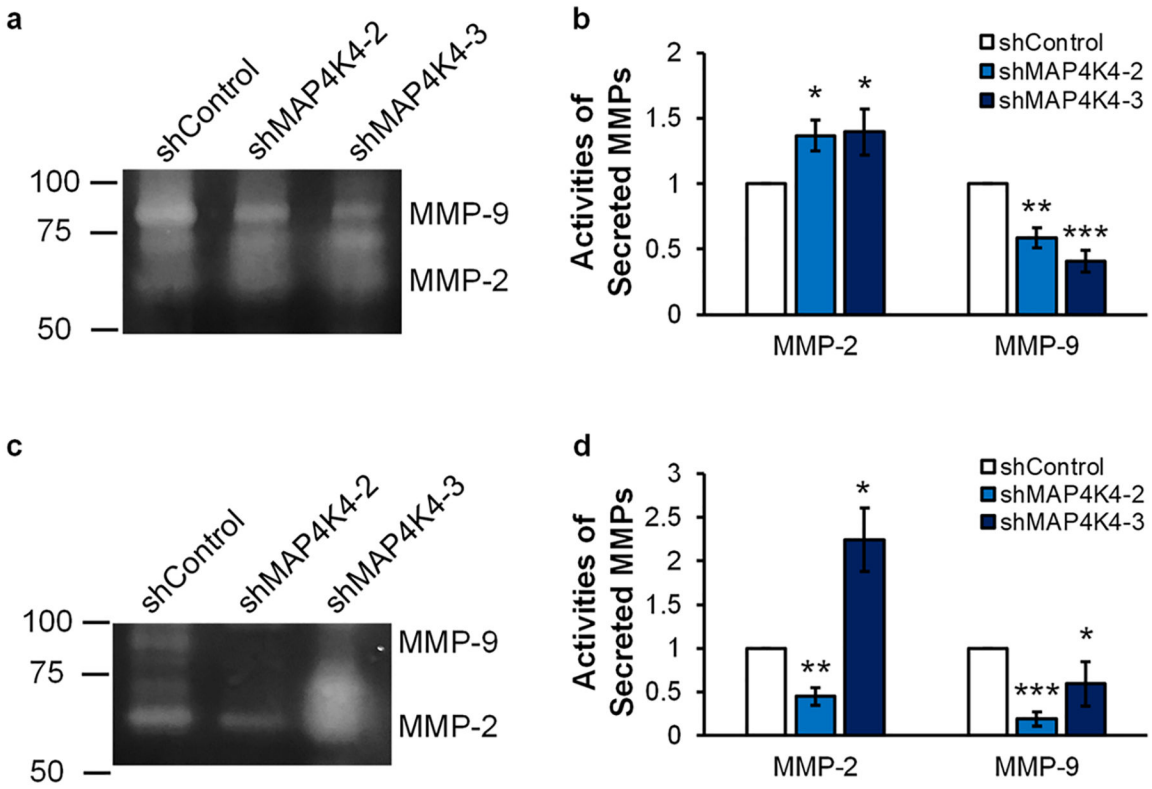

Figure 5.

MAP4K4 regulates the enzymatic activity of secreted MMP-9. (a) Gelatin zymography assay showing the changes in activities of secreted MMP-2 and MMP-9 upon shRNA-mediated stable knockdown of *MAP4K4* gene in PC3 cells. (b) Modulation of activities of secreted MMP-2 and MMP-9 by MAP4K4 in PC3 cells ($n = 3$). (c) Gelatin zymography assay showing the changes in activities of secreted MMP-2 and MMP-9 after shRNA-mediated stable knockdown of *MAP4K4* gene in PC3MLN4 cells. (d) Modulation of activities of secreted MMP-2 and MMP-9 by MAP4K4 in PC3MLN4 cells. The data represent the mean ± SD of the quantification results ($n = 3$). The p values were calculated using an unpaired, two-tailed Student's t-test: #, $p \geq 0.05$; *, $0.01 \leq p < 0.05$; **, $0.001 \leq p < 0.01$; ***, $p < 0.001$.